

# Site Preference Energetics, Fluxionality, and Intramolecular M–H···H–N Hydrogen Bonding in a Dodecahedral Transition Metal Polyhydride<sup>†</sup>

Ramon Bosque, Feliu Maseras, and Odile Eisenstein\*

Laboratoire de Structure et Dynamique des Systèmes Moléculaires et Solides, UMR 5636, Case Courrier 14, Université de Montpellier 2, 34905 Montpellier Cedex 5, France

Ben P. Patel, Wenbin Yao, and Robert H. Crabtree\*

Department of Chemistry, Yale University, 225 Prospect Street, New Haven, Connecticut 06511-8118

Received January 23, 1997<sup>⊗</sup>

Two successive decoalescence events in the hydride region of the <sup>1</sup>H NMR spectrum of [ReH<sub>5</sub>(PPh<sub>3</sub>)<sub>2</sub>(py)] (py = pyridine) are now firmly associated with turnstile and pseudorotation fluxionality mechanisms by eliminating an alternative pairwise mechanism. Ab initio (B3LYP) calculations on ReH<sub>5</sub>(PH<sub>3</sub>)<sub>2</sub>L (L = pyridine) have located the transition state for the turnstile mechanism, which proves to be a second dodecahedral tautomer of the starting complex with the pyridine in the normally unfavorable A site. The fluxional process can therefore be considered as an interconversion of two dodecahedral tautomers, and the barrier for the process is identical with the energy difference of the two tautomers. From a comparison in ReH<sub>5</sub>(PPh<sub>3</sub>)<sub>2</sub>L (L = 2-(acetyl amino)pyridine and 4-(acetyl amino)pyridine), it is clear that having a potentially hydrogen-bonding NH group at the ortho or para positions of the pyridine ring causes an acceleration of the fluxionality, as a result of intramolecular Re–H···H–N hydrogen bonding. The theoretical calculations on ReH<sub>5</sub>(PH<sub>3</sub>)<sub>2</sub>L (L = 2-aminopyridine and 4-aminopyridine) show that the experimental barriers are the result of a compromise between two factors: hydrogen bonding, which lowers the barrier for the 2-amino compound, and H···H repulsion resulting from an excessively close approach of the two H atoms in the transition state, which raises the barrier. This implies that the particular hydrogen-bonding ligands chosen were too rigid for optimal rate acceleration.

## Introduction

Current interest in E–H···H–X (E = transition metal, B; X = N, O, C) hydrogen bonds, in which the hydride ligand acts as an unconventional proton acceptor, has led us to look for applications of the phenomenon in chemical reactivity, where one might anticipate rate acceleration effects and modifications of selectivity.<sup>1,2</sup> As a test of the concept, we recently showed that the rate of hydride fluxionality in ReH<sub>5</sub>(PPh<sub>3</sub>)<sub>2</sub>L (L = 2-(acetyl amino)pyridine, **1**) is accelerated as a result of intramolecular Re–H···H–N hydrogen bonding.<sup>3</sup>

The ReH<sub>5</sub>(PPh<sub>3</sub>)<sub>2</sub>L system (L = N-donor ligand) was selected for this study because the single broad hydride resonance in the room-temperature <sup>1</sup>H NMR spectrum of [ReH<sub>5</sub>(PPh<sub>3</sub>)<sub>2</sub>(py)] (py = pyridine; **2**) undergoes two successive decoalescence events in a convenient temperature range upon cooling (298 to 193 K). We have previously proposed that these two events are associated with two distinct fluxionality mechanisms: pseudorotation and turnstile.<sup>4</sup> We now report further evidence to support these assignments. We also find that incorporating an ortho-NHAc group into the pyridine leads to changes in the fluxionality rates that we ascribe to H···H hydrogen bonds. Understanding the effects of H···H hydrogen bonding on

fluxionality requires us to define the transition states for the two mechanisms which can only be done with the help of quantum chemical studies. We report here ab initio (B3LYP) calculations on ReH<sub>5</sub>(PPh<sub>3</sub>)<sub>2</sub>(L) which show unexpected features of the mechanism.

## Results and Discussion

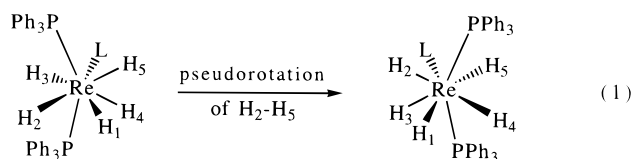
**Hydride Fluxionality in ReH<sub>5</sub>(PPh<sub>3</sub>)<sub>2</sub>(L) Complexes.** Fluxionality is common in many polyhydride complexes, yet in most cases the detailed mechanism of the site exchange is unknown.<sup>5,6</sup> In [ReH<sub>5</sub>(PPh<sub>3</sub>)<sub>3</sub>], the exchange barrier is sufficiently low that separate hydride resonances are observed in the <sup>1</sup>H{<sup>31</sup>P} NMR spectrum only at temperatures below 173 K.<sup>5c</sup> However, in ReH<sub>5</sub>(PPh<sub>3</sub>)<sub>2</sub>(py) (py = pyridine; **2**), the exchange barrier is somewhat higher and two successive decoalescence events are observed upon cooling to 193 K, yielding four singlets in the hydride region of the <sup>1</sup>H{<sup>31</sup>P} NMR spectrum in a 1:2:1:1 integral ratio at the low-temperature limit. The unambiguous assignment of these four resonances by NOE studies and the evidence for the proposed mechanisms for the two fluxional processes have been described in detail elsewhere.<sup>4</sup> The higher temperature process (*T*<sub>C</sub> = 273 K) has been ascribed to a pseudorotation of four of the hydride ligands H<sub>2</sub>–H<sub>5</sub> (eq 1), while the low-temperature process (*T*<sub>C</sub> = 243 K) has been

<sup>†</sup> Dedicated to the memory of Jeremy K. Burdett.

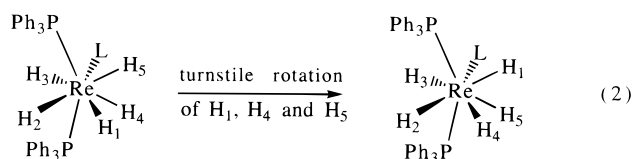
<sup>⊗</sup> Abstract published in *Advance ACS Abstracts*, November 1, 1997.

- (1) Crabtree, R. H.; Eisenstein, O.; Rheingold, A. L.; Koetzle, T. F. *Acc. Chem. Res.* **1996**, *29*, 348.
- (2) Lough, A. J.; Park, S.; Ramachandran, R.; Morris, R. H. *J. Am. Chem. Soc.* **1994**, *116*, 8356.
- (3) Patel, B. P.; Kavallieratos, K.; Crabtree, R. H. *J. Organomet. Chem.* **1997**, *528*, 205.
- (4) Lee, J. C., Jr.; Yao, W.; Crabtree, R. H.; Ruegger, H. *Inorg. Chem.* **1996**, *35*, 695.

- (5) (a) Hlatky, G.; Crabtree, R. H. *Coord. Chem. Rev.* **1985**, *65*, 1. (b) Moore, D. S.; Robinson, S. D. *Chem. Soc. Rev.* **1983**, *12*, 415. (c) Cotton, F. A.; Luck, R. L. *J. Am. Chem. Soc.* **1989**, *111*, 5757.
- (6) Demachy, I.; Esteruelas, M. A.; Jean, Y.; Lledós, A.; Maseras, F.; Oro, L. A.; Valero, C.; Volatron, F. *J. Am. Chem. Soc.* **1996**, *118*, 8388.

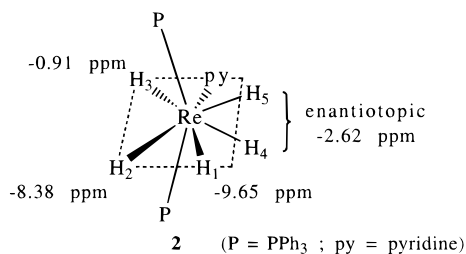


ascribed to a turnstile rotation of three of the hydride ligands H1, H4, and H5 (eq 2). Unfortunately a pairwise exchange



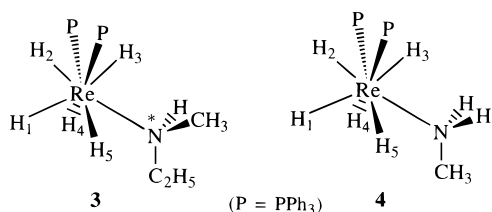
among all three hydrogens could not be excluded in the prior work, but evidence to be described below now supports the turnstile mechanism.

**Turnstile Rotation Mechanism in  $\text{ReH}_5(\text{PPh}_3)_2(\text{L})$  Complexes.** As a result of the plane of symmetry in  $[\text{ReH}_5(\text{PPh}_3)_2(\text{L})]$  complexes, such as **2**, the hydride ligands H4 and H5 are



enantiotopic and therefore chemically equivalent in the low temperature  $^1\text{H}\{^3\text{P}\}$  NMR spectrum, which accounts for the integrated intensity of **2** for the resonance at  $-2.62$  ppm. By introducing an asymmetric center into the complex, we have now broken the symmetry plane and resolved H4 and H5.

Resolution of the H4 and H5 hydride resonances is in principle possible by substitution of the pyridine ligand by a secondary amine, providing the necessary asymmetric center in a location very close to the metal center. We tried the following cases: (a) *N*-methylaniline, (b) *N*-benzylmethylamine, (c) *N*-methyl-*tert*-butylamine, (d) *N*-methylisopropylamine, (e) *N*-ethylmethylamine. The aniline caused decomposition of the starting material  $\text{ReH}_7(\text{PPh}_3)_2$  in the synthesis, and no reaction took place over 48 h in the cases of the bulky alkylamines (b–d); these ligands are presumably too bulky to form stable complexes. Only in the case of *N*-ethylmethylamine were we able to isolate a stable complex,  $[\text{ReH}_5(\text{PPh}_3)_2(\text{NH}(\text{CH}_3)(\text{C}_2\text{H}_5))]$  (**3**). We find that the chirality induced in **3** by the amine indeed



makes H4 and H5 hydrides diastereotopic and therefore chemically inequivalent in the low-temperature (193 K)  $^1\text{H}\{^3\text{P}\}$  NMR spectrum. In addition, decoalescence behavior is found for **3** similar to that previously seen for **2**. Warming the sample from 193 to 213 K initially causes the coalescence of the H4 and H5 resonances, and further warming results in coalescence with the H1 resonance. Both processes have the same barrier, determined from line shape studies, and therefore both refer to the

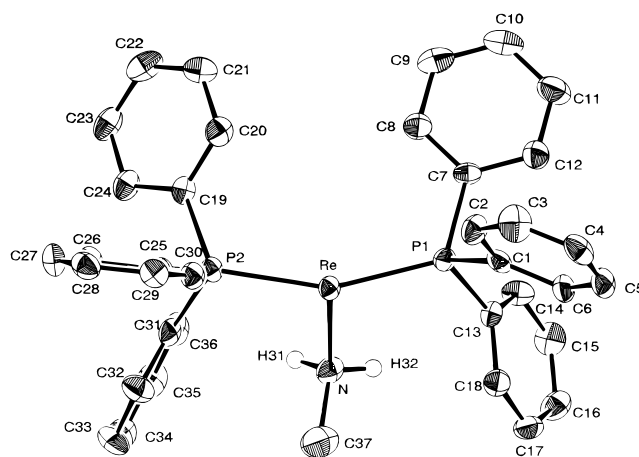


**Figure 1.** ORTEP view of **4** with 50% probability ellipsoids.

**Table 1.** Crystallographic Data for **4**

empirical formula	$\text{C}_{37}\text{H}_{40}\text{NP}_2\text{Re}$
fw	746.9
dimens (mm); habit	0.14, 0.32, 0.39; plate
crystal system	monoclinic
octants collected	$\pm h, -k, +l$
cell determination $2\theta$ range (deg)	10.4–18.0
<i>a</i> (Å)	12.759(3)
<i>b</i> (Å)	15.198(3)
<i>c</i> (Å)	17.347(2)
$\beta$ (deg)	107.61(1)
<i>V</i> (Å <sup>3</sup> )	3206(2)
space group	$P2_1/n$ (No. 14)
<i>Z</i>	4
<i>D</i> <sub>calc</sub> (g/cm <sup>3</sup> )	1.547
<i>F</i> (000)	1496
$\mu$ (Mo $K\alpha$ ) (cm <sup>-1</sup> )	39.64
$\lambda$ (Å)	0.710 69
temp (°C)	-76
no. of reflons	6979 (6756 unique, $R_{\text{int}} = 0.066$ )
<i>R</i>	0.043
<i>R</i> <sub>w</sub>	0.050
GOF	2.18

**Table 2.** Important Bond lengths (Å) and Angles (deg) for  $[\text{ReH}_5(\text{PPh}_3)_2(\text{NH}_2\text{CH}_3)]$  (**4**)

Bond Lengths			
Re–P1	2.351(2)	Re–N	2.253(6)
Re–P2	2.359(2)	N–C37	1.49(1)
Bond Angles			
P1–Re–P2	154.03(7)	P2–Re–N	93.7(2)
P1–Re–N	94.5(2)	Re–N–C37	119.8(5)

same process. These results strongly support the turnstile mechanism over the pairwise exchange alternative.

**Structural Studies.** We needed to verify the ground state structures before we could attempt to assign the transition state structures. Although we were not able to isolate diffraction-quality crystals of **3**, we did manage to do so for the closely related species  $[\text{ReH}_5(\text{PPh}_3)_2(\text{NH}_2\text{CH}_3)]$  (**4**), the primary amine analogue of **3**. The X-ray structure of **4** (Figure 1, Tables 1 and 2) shows the heavy-atom ligands only and not the hydrides. The heavy-atom positions are consistent with a dodecahedral geometry because the bond angles are very close to those previously established for the  $\text{ReH}_5(\text{PR}_3)_3$  unit in neutron diffraction studies of  $\text{ReH}_5(\text{PPh}_3)_3$  and  $\text{ReH}_5(\text{PPh}_2\text{Me})_3$ .<sup>7</sup> Although the hydride ligands were not resolved in the X-ray

(7) (a) Wessel, J.; Lee, J. C., Jr.; Peris, E.; Yap, G. P. A.; Fortin, J. B.; Ricci, J. S.; Sini, G.; Albinati, A.; Koetzle, T. F.; Eisenstein, O.; Rheingold, A. L.; Crabtree, R. H. *Angew. Chem., Int. Ed. Engl.* **1995**, *34*, 2507 (b) Emge, T. J.; Koetzle, T. F.; Bruno, J. W.; Caulton, K. G. *Inorg. Chem.* **1984**, *23*, 4012.

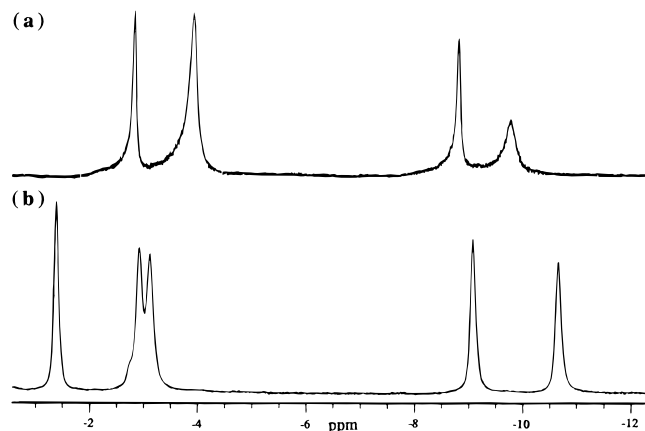


**Figure 2.** Hydride region of the low-temperature (193 K)  $^1\text{H}\{^{31}\text{P}\}$  NMR spectra of **4** (a) and **3** (b).

**Table 3.** Experimental<sup>a</sup> Estimated  $\Delta G^\ddagger$  Barriers for Pseudorotation (at 223 K) and Turnstile (at 193 K) Processes for  $\text{ReH}_5(\text{PPh}_3)_2\text{L}$  (L = 2-(Acetylamino)pyridine, **1**; L = 4-(Acetylamino)pyridine, **5**; L = Pyridine, **2**)

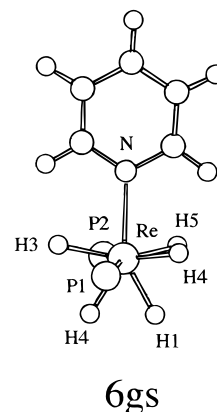
	$\Delta G^\ddagger_{223\text{K}}(\text{pseudorotation})$ (kcal/mol $\pm$ 0.25)	$\Delta G^\ddagger_{193\text{K}}(\text{turnstile})$ (kcal/mol $\pm$ 0.25)
<b>1</b> (ortho)	9.97	8.58
<b>5</b> (para)	9.94	9.30
<b>2</b> (py)	10.40	9.63

<sup>a</sup> The data are presented with two significant figures not because we believe this to represent the error but because differences between the unrounded figures may be of interest, as systematic errors may apply similarly to both data points of a given pair and therefore have less effect on the differences.

experiment, their presence is supported by spectroscopic methods, notably the proton NMR spectrum. In other respects the structure is entirely standard, the phosphine and amine ligands having normal bond lengths and angles. Figure 2 compares the low-temperature  $^1\text{H}\{^{31}\text{P}\}$  NMR spectrum of **4**, where only four hydride resonances can be observed, with that of **3**, in which all five hydride resonances are cleanly resolved.

**Fluxionality Studies on Complexes with Hydrogen-Bonding Ligands.** The hydride resonance in the room-temperature  $^1\text{H}$  NMR spectrum of  $\text{ReH}_5(\text{PPh}_3)_2(2\text{-acetylamino})\text{pyridine}$  (**1**) undergoes the same types of decoalescence events previously seen<sup>4</sup> for  $[\text{ReH}_5(\text{PPh}_3)_2(\text{py})]$ , suggesting that the mechanism of fluxionality is unchanged. The effect of hydrogen bonding on the fluxionality was probed by introducing an  $-\text{NHAc}$  group into the ortho position of the pyridine ring. Since any changes in the decoalescence temperatures of **1** versus the unsubstituted pyridine complex could merely have been due to the electronic effect of the substituent on the pyridine ring, we compared **1** with  $\text{ReH}_5(\text{PPh}_3)_2(4\text{-acetylamino})\text{pyridine}$  (**5**), where the  $-\text{NHAc}$  group is located at the para position. This should give the same electronic effect, but intramolecular hydrogen bonding should no longer be possible. We attempted to prepare the *N*-methyl derivative of **1** for control experiments but were unable to isolate the complex.

Line shape analysis<sup>8</sup> of the spectra in the range  $-40$  to  $-90$   $^\circ\text{C}$  for **1** and **5** (see Experimental Section) allows the  $\Delta G^\ddagger$  values shown in Table 3 to be obtained for both turnstile and pseudorotation pathways. Comparison with the unsubstituted pyridine derivative  $\text{ReH}_5(\text{PPh}_3)_2(\text{py})$  (py = pyridine; **2**) shows that in the substituted pyridine there is a strong electronic effect



**6gs**

**Figure 3.** Optimized structure for  $\text{ReH}_5(\text{PH}_3)_2(\text{py})$ , **6gs**. Selected distances ( $\text{\AA}$ ) and angles (deg): Re–P(1,2) 2.364, Re–N 2.255, Re–H1 1.656, Re–H2 1.662, Re–H3 1.711, Re–H4 1.683; Re–H5 1.683, N–Re–H1 149.24, N–Re–H3 80.27, H1–Re–H2 60.11, P1–Re–P2 154.86, P1(2)–Re–H4(5) 69.99, H4–Re–H5 64.42, Re–N–C (average) 121.00.

of the substituent that leads to a significant acceleration of both fluxionality processes. For the pseudorotation pathway, this effect is dominant because the barrier is independent of the position of substitution. This shows that pseudorotation is not affected by hydrogen bonding.

In contrast, the barrier for the turnstile process is significantly different depending on the location of the  $-\text{NHAc}$  substituent, with the ortho species showing the lower barrier. This indicates that intramolecular  $\text{H}\cdots\text{H}$  hydrogen bonding accelerates the turnstile process.

To rule out intermolecular  $\text{N}-\text{H}\cdots\text{H}-\text{Re}$  interactions as the cause, control experiments at different solute concentrations and with various ratios of **1**:free 2-(acetylamino)pyridine and **5**:free 4-(acetylamino)pyridine were performed. No intermolecular effects on hydride fluxionality were detectable by  $^1\text{H}$  NMR, as was expected, since intermolecular hydrogen bonding is entropically disfavored in solution.

**Other Spectroscopic Data.** The presence of hydrogen bonding in the ortho complex, **1**, but not the para isomer, **5**, is supported by the characteristic broadening and low-energy shift ( $\Delta\nu = 228 \text{ cm}^{-1}$ ) of the  $\nu_{\text{N-H}}$  band in the IR spectrum of a dilute  $\text{CH}_2\text{Cl}_2$  solution of **1**, relative to the  $\nu_{\text{N-H}}$  band of a similarly prepared sample of free 2-(acetylamino)pyridine. For **5**, no broadening or shift to lower energy was observed for  $\nu_{\text{N-H}}$ . Similar IR effects have previously been associated with intermolecular  $\text{Re}-\text{H}\cdots\text{H}-\text{N}$  hydrogen bonding.<sup>9</sup> Furthermore we find that the N–H resonance in the  $^1\text{H}$  NMR spectrum of **1** is shifted downfield by 1.9 ppm relative to the N–H resonance of 2-(acetylamino)pyridine. These observations are characteristic of hydrogens involved both in  $\text{M}-\text{H}\cdots\text{H}-\text{N}$  and in conventional hydrogen bonds.<sup>10</sup>

**Theoretical Study of the Turnstile Mechanism: Dodecahedral Tautomerism.** The geometry of the parent model compound  $\text{ReH}_5(\text{PH}_3)_2(\text{py})$  (**6gs**) (gs = ground state; py = pyridine) has been fully optimized, resulting in a  $C_s$  structure where the mirror plane contains the metal and the pyridine ring (Figure 3). This structure has a dodecahedral geometry,<sup>11</sup> one of the most common polyhedra for eight-coordination.<sup>12</sup> In an ideal dodecahedron, the ligands belong to two orthogonal

(9) Peris, E.; Wessel, J.; Patel, B. P.; Crabtree, R. H. *J. Chem. Soc., Chem. Commun.* **1995**, 2175.

(10) Jeffrey, G. A.; Saenger, W. *Hydrogen Bonding in Biological Structures*; Springer: New York, 1991.

(11) Hoard, J. L.; Silverton, J. V. *Inorg. Chem.* **1963**, *2*, 235.

(12) Drew, M. G. B. *Coord. Chem. Rev.* **1977**, *24*, 179.

(8) (a) Sandstrom, J. *Dynamic NMR Spectroscopy*; Academic Press: New York, 1982. (b) Values of  $\Delta G^\ddagger$  given in ref 4 for the pyridine complex (**2**) were wrong due to a computational error, later corrected in ref 3.

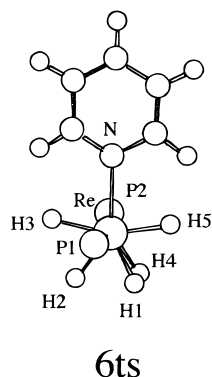
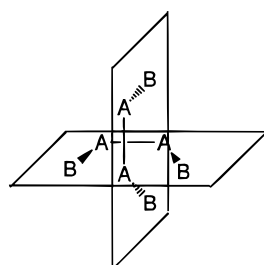


**Figure 4.** Optimized structure for  $\text{ReH}_5(\text{PH}_3)_2(\text{py})$ , **6ts**. Selected distances (Å) and angles (deg): Re–P(1,2) 2.382, Re–N 1.956, Re–H1 1.918, Re–H2 1.904, Re–H3 1.630, Re–H4 1.931, Re–H5 1.727; N–Re–H5 88.00, N–Re–H3 90.09, H2–Re–H3 62.57, H2–Re–H5 119.32, P1–Re–P2 168.21, H1–Re–H4 45.43, P1–Re–H4 65.16, Re–N–C (average) 120.00.

### Chart 1



BAAB trapezoids (Chart 1). The B–M–B angle being much larger than A–M–A, A sites are preferentially occupied by the least bulky ligands. In **6gs**, the two trapezoids are defined by N, H3, H2, H1 and by P1, H4, H5, P2, respectively. The pyridine, the two phosphine ligands, and the H1 hydride ligand occupy the B sites, while the four other hydride ligands occupy the A sites. The preference of hydrides for A sites is a consequence of their small steric size.

The structure of **6gs** (Figure 3) found here is essentially identical to that of  $\text{ReH}_5\text{L}_3$  as given by neutron diffraction (L =  $\text{PMePh}_2$ )<sup>7b</sup> or ab initio calculations<sup>7a,13</sup> (L =  $\text{PH}_3$ ). Nor does the intermolecular hydrogen-bonding modify the geometry around Re as shown by the neutron diffraction data<sup>7a</sup> for  $\text{ReH}_5\text{L}_3 \cdot \text{indole}$  (L =  $\text{PPh}_3$ ). The dodecahedral structure is highly robust to changes of ligand and the presence of  $\text{H} \cdots \text{H}$  bonding. Even the isoelectronic complex  $\text{OsH}_5\text{L}_3^+$  is a similar dodecahedron.<sup>14</sup>

VT NMR studies show a low-barrier turnstile rotation of H1, H4, and H5. In this paper, we were also able to definitely exclude the pairwise process. The theoretical studies support these results: the transition state **6ts** (Figure 4) for the exchange of the three hydrides was successfully located. The structure **6ts** was successfully characterized as a stationary point by its analytically computed zero gradient and identified as a transition state from the presence of a single negative eigenvalue in its Hessian. Although the full Hessian was not computed, the original estimation by the program was improved through numerical calculation of terms involving selected geometrical parameters, precisely those corresponding to the eigenvector with the negative eigenvalue. The transition vector corresponds to the turnstile rotation of the triangle defined by the three

hydride ligands, indicating its connection with **6gs**. This relationship was further confirmed by the fact that **6gs** was the product obtained in a downhill optimization from a geometry generated by a small displacement from **6ts**.

The energy of the transition state **6ts** is 9.02 kcal/mol above the ground state **6gs**, which is in agreement with the experimental value<sup>3</sup> of  $10.40 \pm 0.25$  kcal/mol. We also unsuccessfully sought other transition states, namely those for H4/H5 and H1/H5 pairwise exchanges. Clearly other paths could be imagined for the intermolecular rearrangement of an 8-coordinate hydride, notably ones involving square antiprismatic, bicapped trigonal prismatic, or hexagonal pyramidal geometries, but a systematic search would not be feasible in practice. In initial attempts, by sketching plausible paths on paper, we were not able to devise one by which the *selective* exchange of the three hydrides in question could be achieved via any of these intermediates. Finally, the fact that the calculated energy barrier is close to the experimental one provides strong support for the proposed mechanism. The nature of the transition state **6ts** confirms the preference for a concerted motion of the three hydrogens. Although no symmetry restrictions were imposed during the geometry optimization process, structure **6ts**, like **6gs**, has  $C_s$  symmetry, with the symmetry plane containing the metal and the pyridine ring. No short dihydrogen coordination is found in **6ts** since the shortest  $\text{H} \cdots \text{H}$  (H4–H5) distance is 1.486 Å. The oxidation state of the metal therefore remains unchanged during the hydrogen exchange.

Surprisingly, the transition state structure is a dodecahedral tautomer of the ground state structure in which the py ligand has moved from a B site to an A site, while an H has moved from an A to a B site, as suggested by Gusev and Berke.<sup>15</sup> One way to view the transition structure is to consider the mutual site exchange of H3 and N, but in reality the exchange is the result of a rotation of the triangle consisting of the three H atoms, H1, H4, and H5, to bring the vertex, which lies in the mirror plane, *cis* to pyridine. The two trapezoids in the rearranged dodecahedron are now defined by H5, N, H3, H2 and by P1, H4, H1, P2, respectively, where A sites are occupied by N, H3, H4, H1 and B sites by H5, H2, P1, P2. In contrast to **6gs**, where all the A sites were occupied by hydrides, the pyridine now occupies an A site. Since it is commonly accepted<sup>11,12</sup> that bulky ligands prefer B sites, we consider this placement as the most likely origin for the energy difference between the two structures. In contrast, the direct steric interaction of the phosphine ligands with the pyridine seems to be of lesser importance since we find an activation energy very close to the experimental one even with the model phosphine,  $\text{PH}_3$ . If such steric effects were important, the calculations would have been expected to deviate significantly from experiment. These arguments indicate that the barrier for the turnstile rotation process can be viewed as the energy difference between two isomeric dodecahedra.

If the  $\Delta G^\ddagger$  does indeed represent the energy difference between the two dodecahedral tautomers, then we can say something about electronic effects on site preferences.<sup>3</sup> Prior NMR studies have shown that independent of any H-bonding effects, the energy barrier of the exchange process is decreased by  $\pi$ -donors ( $\Delta G^\ddagger = 9.30$  kcal/mol, X =  $\text{NHAc}$ ) and increased by  $\pi$ -acceptors ( $\Delta G^\ddagger = 10.2$  kcal/mol, X =  $\text{COOCH}_3$ ) in an isosteric series of species of the type  $[\text{ReH}_5(\text{PPh}_3)_2(p\text{-XC}_5\text{H}_4\text{N})]$  containing differently para-substituted pyridines. Calculations with X =  $\text{NH}_2$  and  $\text{COOH}$  were carried out to study this specific substituent effect. In agreement with the experimental trend, a  $\pi$ -donor ( $\text{NH}_2$ ) lowers the barrier (to 7.98 kcal/mol) while a

(13) Kuhlman, R.; Gusev, D. G.; Eisenstein, O.; Caulton, K. G. *J. Am. Chem. Soc.*, submitted for publication.

(14) Maseras, F.; Koga, N.; Morokuma, K. *J. Am. Chem. Soc.* **1993**, *115*, 8313.

(15) Gusev, D. G.; Berke, H. *Chem. Ber.* **1996**, *129*, 1143.

$\pi$ -acceptor ( $X = \text{COOH}$ ) increases the barrier (9.37 kcal/mol) versus that of the unsubstituted pyridine (9.02 kcal/mol). The difference in the computed barriers is small (0.35 kcal/mol), but it reproduces both the sense and the magnitude of the experimental values. The larger lowering of the calculated barrier is coherent with the stronger  $\pi$ -donating effect of  $\text{NH}_2$  versus  $\text{NHAc}$ .

If, as we believe, electronic effects do indeed play the dominant role in determining the barriers for this series of compounds, the results are most easily explained if the site preferences in the dodecahedron depend on the electronic properties of the ligands, electron donors preferring A sites (the location of the pyridine in the transition state) and electron acceptors preferring B sites (the location of the pyridine in the ground state). Never before have two isomeric dodecahedral structures been available for energy comparison, but in this case we suggest that the energy barrier for the turnstile process effectively gives a measure of the energy relationship between the two isomers. In addition to steric factors, which are known to favor placement of bulky ligands in the B site,<sup>11,12</sup> we suggest that A sites, occupied by the pyridine ligand in the transition state, are preferred by the stronger electron-donor pyridines, while B sites, occupied by the pyridine ligand in the ground state, are preferred by the weaker electron-donor pyridines. This seems the most plausible explanation for the behavior, observed both in calculations and in experiments on the systems containing an isosteric series of para-substituted ligands, where donor substituents decrease the barrier size and acceptor substituents increase it. These ideas may help rationalize the structure of other dodecahedral complexes in the future, even if a precise explanation of the precise reasons for these electronic preferences needs further study.

**Theoretical Study of the Effect of Hydrogen Bonding on the Dodecahedral Tautomerism.** Because the transition state for the turnstile mechanism causes one hydride to approach the pyridine, ortho-substitution at the pyridine by  $\text{NH}_2$  can stabilize the transition state by introducing  $\text{H}\cdots\text{H}$  hydrogen bonds, which can lower the activation barrier for exchange.<sup>1,16</sup> Experimental data suggest this interpretation since the exchange barrier in  $\text{ReH}_5(\text{PPh}_3)_2(2\text{-acetylaminopyridine})$  is 0.7 kcal/mol lower than that in the para-substituted system. Theoretical calculations reveal a more complicated situation, however. The ground state (**7gs**) (Figure 5) has a structure similar to that of **6gs**, with a longer  $\text{Re}-\text{N}$  distance (2.293 Å) than in the pyridine complex (2.255 Å). The compound **7gs** has two short  $\text{H}\cdots\text{H}$  contacts of 1.825 Å for  $\text{H}_5-\text{H}_a$  and 1.882 Å for  $\text{H}_4-\text{H}_a$ , corresponding to only moderately strong  $\text{H}\cdots\text{H}$  hydrogen bonds. In this case, however, the exchange reaction does not proceed smoothly, in one single step, but goes instead through an intermediate **7int** (Figure 6) that was characterized as a local minimum since all eigenvalues in the updated Hessian matrix were found to be positive. The intermediate **7int** has no symmetry, and its structure around Re is that of a dodecahedron with *o*- $\text{NH}_2\text{py}$  at the A site (i.e., similar to that of transition state **6ts**). The amine group  $\text{NH}_2$  is approximately coplanar with the pyridine ring, as in **6ts**. The difference between **6ts** and **7int** lies in the dihedral angle between the pyridine ring and the Re, N, and H3 plane. In **6ts**, the dihedral angle is  $0^\circ$ , while a significant twist angle ( $41^\circ$ ) is found in **7int**. In **7int** the  $\text{H}_5-\text{H}_a$  distance is 1.621 Å, a value which is unusually short<sup>1</sup> for nonbonded hydrides and corresponds to a strong  $\text{H}\cdots\text{H}$  interaction, which accounts for the fact that the intermediate **7int** is only 3.72 kcal/mol higher than the ground state, **7gs**. By comparison with that of *p*- $\text{NH}_2\text{py}$ ,

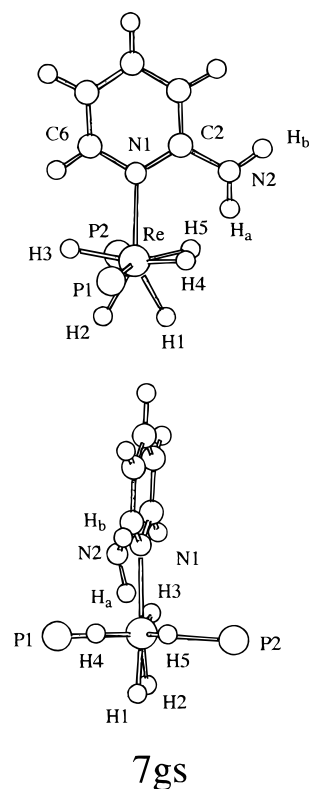


**Figure 5.** Optimized structure for the ground state of  $\text{ReH}_5(\text{PH}_3)_2(2\text{-aminopyridine})$ , **7gs**. Selected distances (Å) and angles (deg):  $\text{Re}-\text{P}$  2.363,  $\text{Re}-\text{N}$  2.293,  $\text{Re}-\text{H}_1$  1.654,  $\text{Re}-\text{H}_2$  1.660,  $\text{Re}-\text{H}_3$  1.704,  $\text{Re}-\text{H}_4(5)$  1.686,  $\text{N}_2-\text{H}_a$  1.036,  $\text{N}_2-\text{H}_b$  1.037,  $\text{H}_a\cdots\text{H}_4$  1.855;  $\text{N}-\text{Re}-\text{H}_1$  150.26,  $\text{N}-\text{Re}-\text{H}_3$  80.12,  $\text{H}_3-\text{Re}-\text{H}_2$ , 70.4,  $\text{H}_1-\text{Re}-\text{H}_2$  59.24,  $\text{P}_1-\text{Re}-\text{P}_2$  152.90,  $\text{H}_4-\text{Re}-\text{H}_5$  69.30,  $\text{P}-\text{Re}-\text{H}_4(5)$  68.69,  $\text{Re}-\text{N}_1-\text{C}_2$  123.7,  $\text{Re}-\text{N}_1-\text{C}_6$  118.80,  $\text{N}_1-\text{C}_2-\text{N}_2$  119.60.

the energy has dropped by 3.76 kcal/mol as a result of hydrogen bonding. In designing the experiment, we had hoped that all of this  $\text{H}\cdots\text{H}$  bond stabilization would be available for transition state stabilization, but the theoretical study suggests that **7int**, where this stabilization is fully present, is only an intermediate on the way to the true transition state. We propose that because the same transition state must exist for forward and back reactions, symmetry arguments require a plane of symmetry to be present in the true transition state; this forces  $\text{H}_5$  and  $\text{H}_a$  to approach very close. The corresponding transition state **7ts** was indeed located and was found to be 7.48 kcal/mol higher than the ground state **7gs**. Considering that the replacement of Ac by H in the calculations has lowered the activation energies by 0.7 kcal/mol, the calculated value for *o*- $\text{NHAc}$  can be estimated as 8.2 kcal/mol, close to the experimental value, 8.6 kcal/mol.

Comparing the structure of the intermediate **7int** (Figure 6) and the transition state **7ts** (Figure 7) helps explain the origin of the unexpectedly high barrier. As mentioned previously, the intermediate already shows significant  $\text{H}\cdots\text{H}$  bonding and trying to force the H atoms even closer together when  $\text{Re}-\text{H}_5$  and  $\text{NH}_a$  become coplanar is therefore somewhat destabilizing. The geometry of the transition state shows evidence of these constraints. The  $\text{H}_5\cdots\text{H}_a$  distance (1.487 Å) is much too short for two nonbonded hydrogens. At the same time the  $\text{Re}-\text{H}_5$  (1.717 Å) and the  $\text{N}-\text{H}_a$  distances (1.047 Å) have shortened with respect to the intermediate (1.723 and 1.053 Å, respectively). In addition, the whole pyridine ring has tilted away from  $\text{Re}-\text{H}_5$  by  $4^\circ$  both around the pyridine N and around the metal. These movements tend to minimize the compressive  $\text{H}\cdots\text{H}$  interaction while retaining the  $\text{Re}-\text{H}$  and  $\text{N}-\text{H}$  bonds. At no point does the complex seem to prefer a structure having an  $\text{H}_2$  molecule trapped between a Re and N atoms. Simple

(16) Richardson, T. B.; deGala, S.; Crabtree, R. H.; Siegbahn, P. E. M. *J. Am. Chem. Soc.* **1995**, *117*, 12875.

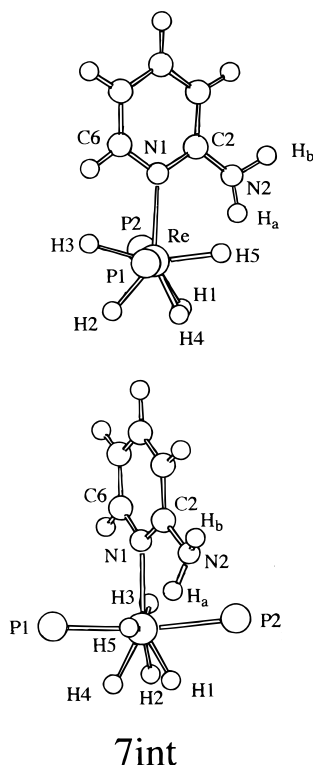


**Figure 6.** Optimized structure for the  $\text{ReH}_5(\text{PH}_3)_2(2\text{-aminopyridine})$  intermediate, **7int**. Selected distances (Å) and angles (deg): Re–P1, 2.271; Re–P2, 2.372; Re–N, 2.271; Re–H1, 1.658; Re–H2, 1.661; Re–H3, 1.710; Re–H4, 1.648; Re–H5, 1.723; N2–H<sub>a</sub>, 1.053; N2–H<sub>b</sub>, 1.048; H<sub>a</sub>···H5, 1.621; H5–Re–H2, 137.43; N–Re–H5, 79.92; N–Re–H3, 76.97; H3–Re–H2, 65.83; P1–Re–P2, 166.06; P1–Re–H4, 68.55; P1–Re–H1, 69.91; Re–N1–C2, 121.21; Re–N1–C6, 120.57; N1–C2–N2, 118.08; C2–N2–H<sub>a</sub>, 111.21.

thermodynamic considerations for the relative bond energies of Re–H, N–H, and H<sub>2</sub> suggest that such a process is unlikely.

## Conclusions

The results show that the favorable effect of the hydrogen bond on lowering the barrier has been partially offset by the necessity to force H5 and H<sub>a</sub> in **7ts** into too close contact. If the system were slightly more flexible, the full potential of the H···H bond could be expressed in the transition state and a lower activation energy would be obtained. It is the requirement for a plane of symmetry in the transition state that causes the problems, and in future applications to other chemical reactivity problems, we expect to use a more flexible system which will be able to rearrange sufficiently to allow strong stabilization of the transition state and therefore show large rate accelerations. This finding is consistent with the commonly accepted principle<sup>17</sup> of biochemistry that flexibility of a protein is an important requirement for catalytic activity. It is also shown that, in these pentahydrides, the turnstile exchange process consists of a tautomerism between the ground state dodecahedron and a transition state dodecahedron where the pyridine ring has exchanged places with an adjacent A site hydride. The pseudorotation pathway is insensitive to the presence of the 2-NHAc functionality.

## Experimental Section

**General Considerations.** All reactions were carried out under nitrogen using standard Schlenk techniques. Reagent grade benzene and hexanes were refluxed over CaH<sub>2</sub> and degassed prior to use.

(17) Stryer, L. *Biochemistry*, 3rd ed.; Freeman & Co.: New York, 1988; p 220.

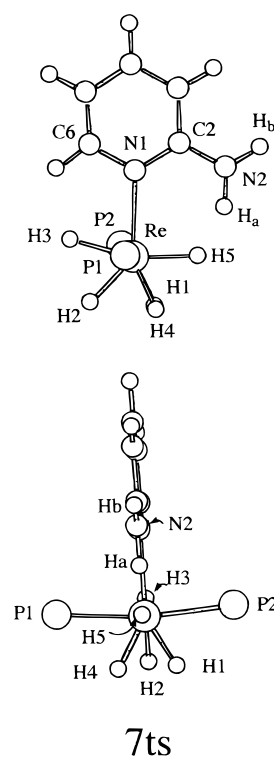


**Figure 7.** Optimized structure for the  $\text{ReH}_5(\text{PH}_3)_2(2\text{-aminopyridine})$  transition state, **7ts**. Distances (Å) and angles (deg): Re–P, 2.366; Re–N, 2.317; Re–H1, 1.652; Re–H2, 1.652; Re–H3, 1.705; Re–H4, 1.652; Re–H5, 1.717; N2–H<sub>a</sub>, 1.047; N2–H<sub>b</sub>, 1.038; H5···H<sub>a</sub>, 1.487; H5–Re–H2, 139.85; H5–Re–N, 86.49; N–Re–H3, 75.79; H3–Re–H2, 62.77; P1–Re–P2, 165.59; P1–Re–H4, 69.08; H1–Re–H4, 54.55; Re–N1–C2, 124.16; Re–N1–C6, 118.56; N1–C2–N2, 119.20; C2–N2–H<sub>a</sub>, 117.37.

*N*-Methylethylamine (Aldrich) and *N*-methylamine (Matheson) were used as received.  $\text{ReH}_7(\text{PPh}_3)_2$  was prepared according to a literature procedure.<sup>18</sup> IR spectra were recorded on a Midac M1200 FTIR spectrometer. <sup>1</sup>H and <sup>31</sup>P NMR were recorded on a GE Omega 300 MHz spectrometer (operating at 121.7 MHz for <sup>31</sup>P). C, H, and N elemental analyses were obtained from Atlantic Microlabs, Norcross, GA.

**Preparation of  $[\text{ReH}_5(\text{PPh}_3)_2(\text{NH}(\text{CH}_3)(\text{C}_2\text{H}_5)]$  (**3**).**  $\text{ReH}_7(\text{PPh}_3)_2$  (181 mg, 0.252 mmol) was stirred with *N*-ethylmethylamine (1.0 mL, 11.7 mmol) in benzene (20 mL) at ambient temperature for 48 h, during which the color changed from pale to bright yellow. The solution was filtered through Celite, the volume of the filtrate was reduced to 3 mL under reduced pressure, and hexanes (10 mL) were slowly added to precipitate a bright yellow solid. The product was filtered off, washed with hexanes, and dried in vacuo (105 mg, 54%). The product was recrystallized from  $\text{CH}_2\text{Cl}_2/\text{Et}_2\text{O}$ . <sup>1</sup>H NMR ( $\text{CD}_2\text{Cl}_2$ , 298 K):  $\delta$  7.73 (12H, br s, Ph), 7.30 (18H, br s, Ph), 2.35 (1H, s, NH), 1.73 (3H, br s,  $\text{NCH}_3$ ), 1.49 (2H, br s,  $\text{NCH}_2\text{CH}_3$ ), 0.07 (3H, br s,  $\text{NCH}_2\text{CH}_3$ ), –4.85 (5H, br s, ReH). <sup>1</sup>H NMR ( $\text{CD}_2\text{Cl}_2$ , 183 K):  $\delta$  7.63 (12H, br s, Ph), 7.25 (18H, br s, Ph), 2.26 (1H, s, NH), 1.66 (3H, br s,  $\text{NCH}_3$ ), 1.25 (2H, br s,  $\text{NCH}_2\text{CH}_3$ ), –0.12 (3H, br s,  $\text{NCH}_2\text{CH}_3$ ), –1.38 (1H, t, <sup>2</sup>*J*<sub>H–P</sub> = 27.2 Hz, Re–H<sub>3</sub>), –2.91 (1H, d, <sup>2</sup>*J*<sub>H–P</sub> = 25.3 Hz, Re–H<sub>4/5</sub>), –3.11 (1H, d, <sup>2</sup>*J*<sub>H–P</sub> = 27.2 Hz, Re–H<sub>5/or4</sub>), –9.07 (1H, t, <sup>2</sup>*J*<sub>H–P</sub> = 19.5 Hz, Re–H<sub>2</sub>), –10.64 (1H, br s, Re–H<sub>1</sub>). <sup>31</sup>P NMR ( $\text{CD}_2\text{Cl}_2$ , 298 K):  $\delta$  48.32 (br s). IR (thin film):  $\nu_{\text{N–H}}$  3276 (m),  $\nu_{\text{Re–H}}$  2011 (m), 1959 (w), 1907 (m), 1859 (m). Anal. Calc for  $\text{C}_{39}\text{H}_{44}\text{NP}_2\text{Re}\cdot 3\text{H}_2\text{O}$ : C, 56.51; H, 5.98; N, 1.69. Found: C, 56.49; H, 5.40; N, 1.79.

**Preparation of  $[\text{ReH}_5(\text{PPh}_3)_2(\text{NH}_2\text{CH}_3)]$  (**4**).**  $\text{ReH}_7(\text{PPh}_3)_2$  (100 mg, 0.14 mmol) was dissolved in freshly distilled benzene (20 mL) at room temperature. *N*-Methylamine was bubbled through the solution for 30 min, during which the color changed from pale brown to pale yellow. The flask was filled with 1 atm of *N*-methylamine gas, and the contents were stirred for an additional 18 h. The resulting bright yellow solution

(18) Chatt, J.; Coffey, R. S. *J. Chem. Soc. A* **1969**, 1963.

was filtered through Celite, the volume of the filtrate was reduced to 3 mL under reduced pressure, and hexanes (20 mL) were slowly added to precipitate a yellow solid, which was recrystallized from CH<sub>2</sub>Cl<sub>2</sub>/Et<sub>2</sub>O, washed with copious amounts of hexanes, and dried under vacuum (90 mg, 87%). <sup>1</sup>H NMR (CD<sub>2</sub>Cl<sub>2</sub>, 298 K): δ 7.70 (12H, br, Ph), 7.28 (18H, br, Ph), 1.26 (3H, br, NCH<sub>3</sub>), 0.919 (2H, br, NH<sub>2</sub>), -5.527 (5H, br s, ReH). <sup>1</sup>H{<sup>31</sup>P} NMR (CD<sub>2</sub>Cl<sub>2</sub>, 193 K): δ 7.70 (12H, br, Ph), 7.28 (18H, br, Ph), 1.26 (3H, br, NCH<sub>3</sub>), 0.919 (2H, br, NH<sub>2</sub>), -2.794 (1H, s, Re-H<sub>2</sub>), -3.882 (2H, s, Re-H<sub>4</sub> and Re-H<sub>5</sub>), -8.746 (1H, s, Re-H<sub>2</sub>), -9.694 (1H, s, Re-H<sub>1</sub>). <sup>31</sup>P NMR (CD<sub>2</sub>Cl<sub>2</sub>, 298 K): δ 47.47 (br s). IR (Nujol): ν<sub>N-H</sub> 3337 (m), ν<sub>Re-H</sub> 2048 (m), 2013(s), 1921 (m), 1836(s). Anal. Calc for C<sub>37</sub>H<sub>40</sub>NP<sub>2</sub>Re·2H<sub>2</sub>O: C, 56.78; H, 5.63; N, 1.79. Found: C, 56.94; H, 5.22; N, 2.09.

**NMR Studies.** Line shape studies were carried out as follows. The natural linewidth was estimated from the <sup>1</sup>H{<sup>31</sup>P} NMR spectra at -90 °C with 5 Hz being subtracted to account for unresolved <sup>2</sup>J(H,H<sub>2</sub>) couplings evident in the COSY experiment of ref 4. Initial broadening was evident in all three complexes at -80 °C, and the rate constant for exchange was calculated from the usual<sup>8</sup> formula. We used the line broadening for H1 because this hydrogen always leaves its site during the low-temperature process. The ΔG<sup>‡</sup> at -80 °C was calculated from the rate constants for all three complexes from the standard formula.<sup>8</sup> Line shape studies for the higher temperature process were carried out in the same way but at -50 °C.

**Crystallography.** Pale yellow crystals of **4** were grown from a solution of benzene and hexanes in an NMR tube at 5 °C. A single crystal having approximate dimensions of 0.14 × 0.32 × 0.39 mm was mounted on a glass fiber. All measurements were made on an Enraf-Nonius CAD-4 diffractometer with graphite monochromated Mo Kα radiation to a 2θ<sub>max</sub> of 52.6°. The structure was solved by the Patterson method.<sup>19a</sup> The non-hydrogen atoms were refined anisotropically. The hydrogen atoms were included in calculated positions. In the case of the methyl group, one hydrogen atom was located in the difference map and included at an idealized distance to set the orientation of the other two hydrogen atoms. In the case of the NH<sub>2</sub> group, the hydrogen atoms were originally located in the difference map, but failed to refine satisfactorily and therefore were included in calculated positions. The final cycle of full-matrix least-squares refinement was based on 4786 observed reflections (*I* > 3.00σ(*I*)) and 370 variable parameters and converged with unweighted and weighted factors of

$$R = \sum ||F_o| - |F_c|| / \sum |F_o| = 0.043$$

$$R_w = [ \sum w(|F_o| - |F_c|)^2 / \sum wF_o^2 ]^{1/2} = 0.050$$

Neutral-atom scattering factors were taken from Cromer and Waber.<sup>19b</sup> Anomalous dispersion effects were included in *F<sub>c</sub>*.<sup>20</sup> All calculations were performed using the TEXSAN<sup>21</sup> crystallographic software package of the Molecular Structure Corp.

**Computational Details.** Ab initio calculations on the model systems ReH<sub>5</sub>(PH<sub>3</sub>)<sub>2</sub>(NC<sub>5</sub>H<sub>4</sub>R)] (R = H, 4-COOH, 4-NH<sub>2</sub>, 2-NH<sub>2</sub>) were performed at the DFT (Becke3LYP) computational level<sup>22</sup> using the Gaussian 94 package<sup>23</sup> of programs. An effective core potential was used to replace the 54 innermost electrons of Re and the 10 innermost electrons of P.<sup>24</sup> The associated basis set LANL2DZ which is a valence double-ζ quality basis was used for Re and P.<sup>24</sup> All atoms bonded to the metal (N, H) are also described by a valence double-ζ basis set (6-31G).<sup>25</sup> A polarization function was added to the hydrides (6-31G\*\*).<sup>26</sup> Atoms not bonded to the metal are represented with a minimal basis STO-3G basis set.<sup>27</sup> Geometry optimizations were carried out without symmetry constraints unless otherwise mentioned.

**Acknowledgment.** We thank the NSF, the CNRS, the Université de Montpellier 2, and the Région Languedoc-Roussillon for support. F.M. thanks the CNRS for a research associate position, R.B. thanks the Ministerio de Educacion for a postdoctoral fellowship, and R.H.C. thanks the NSF for funding and Susan de Gala and Konstantinos Kavallieratos for valuable help.

**Supporting Information Available:** Listings of complete bond distances and angles, all positional and displacement parameters, and anisotropic thermal parameters for **4** (10 pages). Ordering information is given on any current masthead page.

IC970084L

- (19) (a) SHELXS: Sheldrick, G. M.; Egert, E. General Direct Methods and Automatic Patterson. University of Goettingen. (b) Cromer, D. T.; Waber, J. T. *International Tables for X-ray Crystallography*; Kynoch Press: Birmingham, England, 1974; Vol. IV, Table 2.2A.
- (20) Ibers, J. A.; Hamilton, W. C. *Acta Crystallogr.* **1964**, *17*, 781.
- (21) TEXSAN-TEXRAY Structure Analysis Package; Molecular Structure Corp.: The Woodlands, TX, 1989.
- (22) (a) Becke, A. D. *J. Chem. Phys.* **1993**, *98*, 5648. (b) Lee, C.; Yang, W.; Parr, R. G. *Phys. Rev. B* **1988**, *37*, 785.
- (23) Frisch, M. J.; Trucks, G. W.; Schlegel, H. B.; Gill, P. M. W.; Johnson, B. G.; Robb, M. A.; Cheeseman, J. R.; Keith, T.; Petersson, G. A.; Montgomery, J. A.; Raghavachari, K.; Al-Laham, M. A.; Zakrzewski, V. G.; Ortiz, J. V.; Foresman, J. B.; Peng, C. Y.; Ayala, P. Y.; Chen, W.; Wong, M. W.; Andres, J. L.; Replogle, E. S.; Gomperts, R.; Martin, R. L.; Fox, D. J.; Binkley, J. S.; Defrees, D. J.; Baker, J.; Stewart, J. P.; Head-Gordon, M.; Gonzalez, C.; Pople, J. A. *Gaussian 94*; Gaussian, Inc.: Pittsburgh, PA, 1995.
- (24) (a) Hay, P. J.; Wadt, W. R. *J. Chem. Phys.* **1985**, *82*, 284. (b) Wadt, W. R.; Hay, P. J. *J. Chem. Phys.* **1985**, *82*, 299.
- (25) Hehre, W. J.; Ditchfield, R.; Pople, J. A. *J. Chem. Phys.* **1972**, *56*, 2257.
- (26) Krishnan, R.; Binkley, J. S.; Seeger, R.; Pople, J. A. *J. Chem. Phys.* **1980**, *72*, 650.
- (27) Hehre, W. J.; Stewart, R. F.; Pople, J. A. *J. Chem. Phys.* **1969**, *51*, 2657.